

Article

Multi-AUV Control Method Based on Inverse Optimal Control of Integrated Obstacle Avoidance Algorithm

Gang Shao ^{1,2,3,4,*} , Lei Wan ¹ and Huixi Xu ^{2,3,4}

¹ National Key Laboratory of Science and Technology on Underwater Vehicle, Harbin Engineering University, Harbin 150001, China; wanlei@hrbeu.edu.cn

² State Key Laboratory of Robotics, Shenyang Institute of Automation, Chinese Academy of Sciences, Shenyang 110016, China; xhx@sia.cn

³ Institutes for Robotics and Intelligent Manufacturing, Chinese Academy of Sciences, Shenyang 110169, China

⁴ Key Laboratory of Marine Robotics, Shenyang 110169, China

* Correspondence: shaogang@sia.cn

Abstract: Under complex underwater conditions, multiple AUVs work in one area and they need to cooperate for complicated missions. In this study, a design method was applied for multiple autonomous underwater vehicles (AUVs) that are distributed in an area and suddenly receive a command. Using this method, the AUVs work according to their own state and reach the target while avoiding obstacles automatically in the process of collection. A new optimal control method is proposed that achieves the consensus of multiple AUVs as well as offering obstacle avoidance capability with minimal control effort. A non-quadratic obstacle avoidance cost function was constructed from the perspective of inverse optimal control. The distributed analytic optimal control law depends only on the local information that can be generated by the communication topology, which guarantees the proposed behavior, so that the control law does not require information from all AUVs. A simulation and an experiment were performed to verify the consensus and obstacle avoidance effect.

Keywords: multiple AUVs; consensus algorithm; optimal control; obstacle avoidance



Citation: Shao, G.; Wan, L.; Xu, H. Multi-AUV Control Method Based on Inverse Optimal Control of Integrated Obstacle Avoidance Algorithm. *Appl. Sci.* **2023**, *13*, 12198. <https://doi.org/10.3390/app132212198>

Academic Editor: Zaopeng Dong

Received: 12 October 2023

Revised: 3 November 2023

Accepted: 5 November 2023

Published: 10 November 2023



Copyright: © 2023 by the authors. Licensee MDPI, Basel, Switzerland. This article is an open access article distributed under the terms and conditions of the Creative Commons Attribution (CC BY) license (<https://creativecommons.org/licenses/by/4.0/>).

1. Introduction

The development of human society is inseparable from the exploitation and use of various resources. With land resources being gradually exhausted, attention has been turned towards the deep ocean. Numerous manganese nodules, deep-sea oil and gas, hydrothermal deposits, and gas hydrates exist in the submarine world. Thus, the efficient and safe exploration of such resources has become an urgent matter. Autonomous underwater vehicles (AUVs) are an auxiliary intelligent tool for ocean exploration, which play a key role in the application of ocean environment observation [1,2], seabed geomorphology measurement [3], and military reconnaissance [4].

Owing to their power, cable-free autonomy, good masking performance, and wide search range, AUVs offer very wide application prospects in both the civil marine and coastal defense military fields. In particular, AUVs are essential in deep-sea underwater searching. As early as 1963, the “Alvin” and “Kov” underwater robot cooperation of the US to search for and salvage a lost hydrogen bomb in the Spanish trench was a successful case. In early 2014, the US used the “Bluefin Tuna” AUV to conduct a large-scale underwater search at a depth of 4500 m in the Indian Ocean for the missing Malaysia Airlines flight MH370.

Ocean Infinity, which was founded in the US in 2017, has rapidly expanded into a leading global maritime technology company. In early 2020, Ocean Infinity launched Armada, which is a new ship technology and data company, and introduced fleet robotics. The Armada fleet can carry ROVs (remote operated vehicles) and AUVs, as well as a variety of other sensors or equipment, thereby replacing traditional support vessels for seabed

mapping, oil field material transport, subsea construction support, salvage and rescue, military, and other activities.

In 2011, researchers at the Ganz Artificial Life Lab in Austria unveiled the largest cluster of underwater unmanned vehicles in the world at the time: the CoCoRo AUV cluster. The project, which was funded by the European Union and led by Thomas Schmickl, consisted of 41 AUVs that could work together to accomplish tasks, with the main purpose of being used for underwater monitoring and searching. The cluster system was scalable, reliable, and flexible in terms of its behavioral potential. The researchers studied collective self-knowledge through experiments that were inspired by behavioral and psychological science, thereby allowing for the quantification of collective self-knowledge.

Furthermore, the European Commission supported a project known as Smart and Networking Underwater Robots in Cooperation Meshes. The aim was to select, combine, and integrate different and heterogeneous communication technologies, components, and solutions to achieve the best performance for the management and control of underwater vehicles when the robots completed different missions and tasks. This project was completed by testing it in the sea.

With the increasing complexity of AUV search tasks, multi-AUV (MAUV) systems have become an important research direction in the development of underwater vehicles when it is difficult for a single AUV to complete a task. MAUV systems can provide more solutions with higher work efficiency, a higher intelligence level, and better fault tolerance compared to single-AUV systems.

MAUV systems (also known as swarm agents) have mainly arisen owing to limited technology, as the intelligence of a single agent cannot be extended. Thus, it is hoped that coordination and cooperation among multiple agents can deal with complex tasks that a single agent cannot handle. This concept has received significant attention in the scientific research and engineering circles [5,6].

The consensus problem at the center of MAUV cooperative control has been developed over the past several years using various methods. The consensus of the system requires a suitable control protocol to be designed so that all agents can converge to a common value under the premise that they can only exchange information with their neighbors [7]. The consensus performance is obviously affected by the dynamics of the agents and network topology. Numerous results have been studied considering these two factors [8–13]. However, in physical and engineering systems, the consensus problem is expected to ensure that all agents can converge in a certain trajectory to achieve the desired goal. Rapid convergence can be achieved by designing a consensus algorithm to determine the optimal weight matrix [14]. An appropriate function was constructed by maximizing the second smallest eigenvalue of the Laplacian operator, thereby optimizing the consensus algorithm [15]. Furthermore, the average consensus problem was realized by developing an optimal interaction graph [16]. In another study, the consensus problem was expressed as an optimization problem using the linear matrix inequality method [17]. An optimal linear consensus algorithm based on the linear quadratic adjuster has also been proposed [18].

The cooperative mission was studied by [19], analyzing the approach to solve the averaging problem through the application of assumptions that were based on linear iterative form. In [20], each group member interacted with its neighboring states by a linear stochastic matrix until all of them reached the same limit. In [21], a distributed algorithm was generalized for the consensus in fixed topology. In [22], an arranged motion of particulars in a group was controlled by a specific model in order to update the information from the closest neighbor. An optimistic optimization approach with simple black box was devised in a form of a non-linear structure for controlling the agents' behavior in [23].

This research focuses on the analysis of consensus models, the design of consensus protocols, convergence, equilibrium, and application prospects. Many scholars have applied different model methods and carried out in-depth research and expansion of consensus theory from different directions. The consensus has developed rapidly and yielded fruitful results and has been widely applied to a variety of scientific and engineering problems,

including synchronization of coupled oscillators, formation control, swarm control, optimal cooperative control, clustering, sensor networks, etc. [24,25].

In [26] the problem of consensus in multi-AUV recovery systems with time varying delays was explored. A new consensus control protocol for formations was proposed. In [27] the problem of multi-AUV formation control under constraints such as bounded communication delays and nonconvex control inputs was studied. In [28] an improved event-triggering mechanism to coordinate the communication in heterogeneous AUVs was explored. In [29], some effective criteria for consensus of a class of non-smooth opinion dynamics over a directed graph were presented. In [30] the integral sliding mode control protocol was proposed to address the formation control of multi-robot systems. In [31] the output consensus issue for linear multi-agent systems was addressed. It is clear that the convergence time of the system depends on the initial conditions.

Coordination among multiple agents is critical, but the obstacle avoidance strategies that were designed previously neither considered the optimality nor the interaction topology (consensus) issues.

The contributions of this paper are described as follows.

(1) A new consensus algorithm was studied for the single-integrator systems in an obstacle environment. (2) A novel control approach was developed to achieve multi-AUV consensus and have the minimal obstacle avoidance cost. (3) A novel nonquadratic obstacle avoidance cost function was constructed by an inverse optimal control approach. (4) The theory in this paper was verified by practical experiments.

The remainder of this paper is organized as follows: In Section 2, background knowledge on graph theory is presented. The consensus problem is established in Section 3. In Section 4, the main research of this study is outlined. The simulation and data analysis is presented in Section 5. The preliminary verification of the method using an experiment with two AUVs is described in Section 6. Finally, in Section 7, the conclusions are presented.

2. Background Knowledge

Several symbols, definitions, and concepts in graph theory are described in this section. The information that is exchanged in MAUVs is modeled using a directed or undirected graph.

A directed graph can be represented by $G = (N, E)$, where N indicates a finite non-empty set of nodes and E denotes an edge set of ordered pairs of nodes. A directed path is a sequence of ordered edges in the form $(i_1, i_2), (i_2, i_3)$, where $i_j \in N$. For example, $(i_1, i_2) \in E$ indicates that AUV i_2 obtains information from AUV i_1 . The $(i_1, i_2) \in E$ in an undirected graph is unordered.

A non-negative adjacency matrix is constructed:

$$\mathbf{adj} = [\mathbf{adj}_{ij}],$$

where \mathbf{adj} expresses the net topology of the MAUV. In the matrix $\mathbf{adj}_{ii} = 0$, $\mathbf{adj}_{ij} = 1$ if $(j, i) \in E$ and $\mathbf{adj}_{ii} = 0$ if $(j, i) \notin E$, where $i \neq j$.

According to previous work [21], the adjacency matrix is symmetric, i.e., $\mathbf{adj}_{ij} = \mathbf{adj}_{ji}$, $\forall i \neq j$ for the undirected graph. Thus, the Laplacian matrix L of graph G can be defined as follows:

$$L = \Delta - \mathbf{adj} \tag{1}$$

where $\Delta = \text{diag}(\mathbf{adj} \cdot \mathbf{1})$ is the degree matrix of G with diagonal elements $d_i = \sum_j \mathbf{adj}_{ij}$, where $\mathbf{1}$ indicates that all column vectors are 1 and 0 means that they are all 0.

When the graph is connected based on undirected information, L will have a simple zero eigenvalue with an associated eigenvector $\mathbf{1}$ and all other eigenvalues are positive. As L is positive semidefinite, it exhibits the property of

$$L \cdot \mathbf{1} = \mathbf{0} \tag{2}$$

In this study, the main results are derived using this formulation.

3. Problem Specification

The AUV has a single-integrator dynamics model that is expressed as follows:

$$\dot{x}_i = u_i, i = 1, \dots, n \tag{3a}$$

or in the form of matrix

$$\dot{X} = U \tag{3b}$$

where

$$X = [x_1^T, \dots, x_n^T]^T, U = [u_1^T, \dots, u_n^T]^T,$$

in which $x_i(t) \in \mathbb{R}^m$ is the state of the i th AUV, $u_i(t) \in \mathbb{R}^m$ are the control inputs of the i th AUV, $X \in \mathbb{R}^{nm}$ are the aggregate states of all AUVs, and $U \in \mathbb{R}^{nm}$ are the control inputs of all AUVs.

Figure 1 depicts multiple AUVs that are distributed in the sea, the biggest AUV can provide power and all the AUVs can exchange data. In this figure, different colors represent the changes of water depth. MAUV systems can generally reside on the seabed for a long time. When marine geological disasters occur, an AUV will sense the occurrence of the disasters and automatically identify possible disaster sites to evaluate the overall environment. When the system senses an unusual change in the environment, the AUVs will cooperate, and in this phase, they sense the nearby AUVs through the sensors that they carry and determine the location of the collection through negotiation.

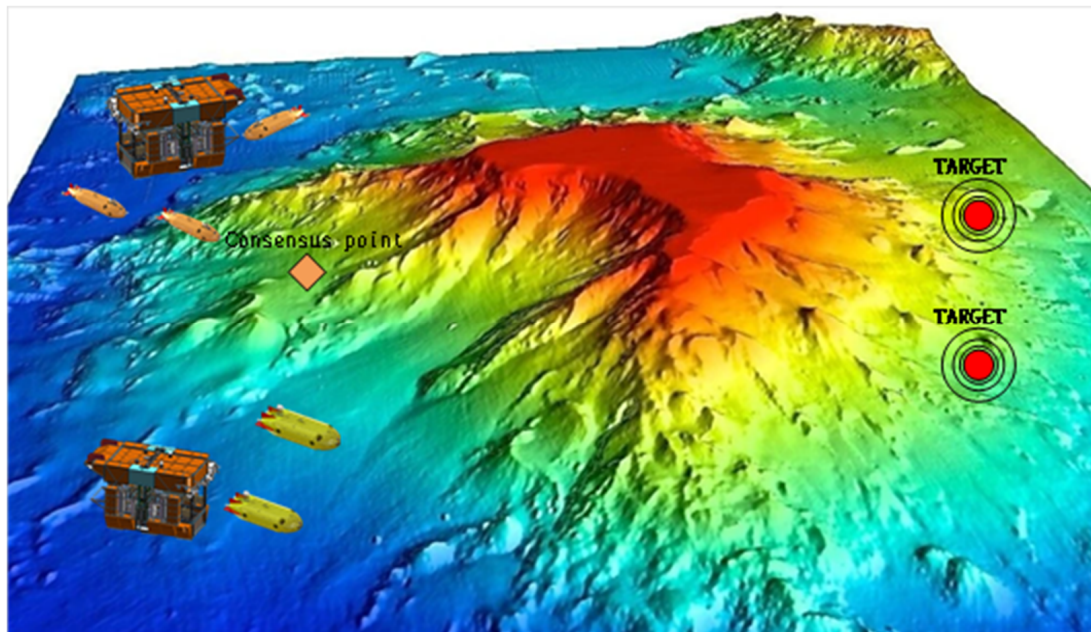


Figure 1. MAUV multi-water area search scenario.

In this study, the consensus problem involves the design of a distributed control law $u_i(t)$ that depends on the information exchange topology such that the states of all AUVs converge to the same value, i.e., $\|x_i(t) - x_j(t)\| \rightarrow 0$. Furthermore, it is guaranteed that obstacles along the AUV trajectory can be avoided.

Figure 2 depicts an example scene of the consensus problem with five AUVs and one obstacle. Three zones are established: the collision, the diagnostic, and the reaction zones, which are defined as follows.

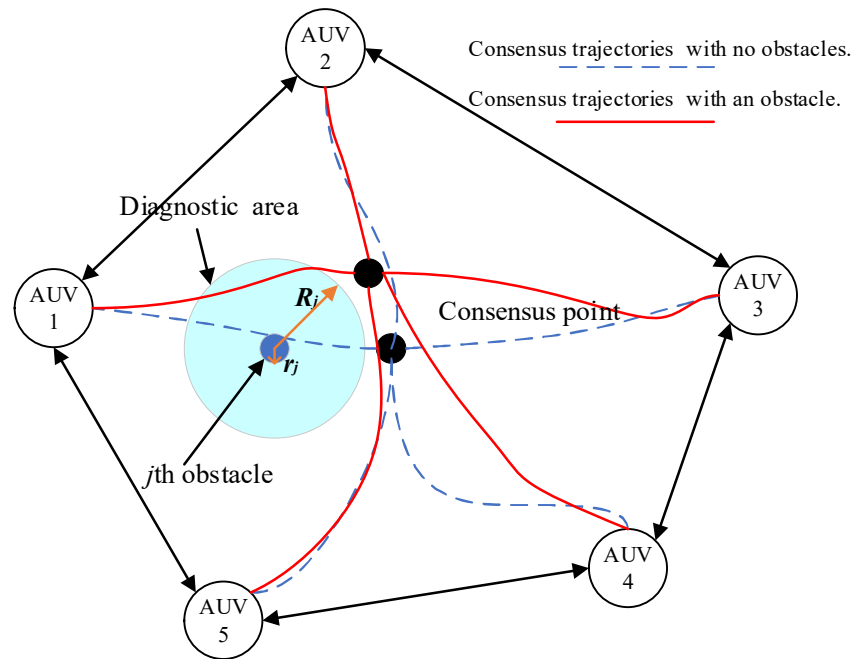


Figure 2. MAUV consensus scene with an obstacle.

Collision zone for the j th obstacle: $\Lambda_j \triangleq \{x|x \in \mathbb{R}^m, \|x - O_{bj}\| \leq r_j\}$. The AUV absolutely cannot enter the interval and each obstacle is solid.

Diagnostic zone for the j th obstacle: $\Psi_j \triangleq \{x|x \in \mathbb{R}^m, \|x - O_{bj}\| \leq R_j\}$. This is the range within which the AUV can detect only one obstacle. Outside this area is the AUV safe area, within which the AUV navigates according to coordinated commands.

Reaction zone for the j th obstacle: $\Gamma_j \triangleq \{x|x \in \mathbb{R}^m, r_j < \|x - O_{bj}\| \leq R_j\}$. In this area, the AUV can sense and avoid obstacles.

Where r_j means the radius of the obstacle, R_j means the range that the AUV can detect the obstacle.

Accordingly, the entire safety area can be represented as $\Theta = (\cup_j \Lambda_j)^c$ and the entire outside diagnostic zone can be represented as $\Pi = (\cup_j \Psi_j)^c$. The symbol \cup and superscript c indicate the union and complement of sets, respectively.

The following three assumptions are included in this study:

A1. All obstacles can be modeled as spheroidal objects.

A2. $\Psi_j \cap \Psi_k = \emptyset, j \neq k$.

A3. It is assumed that the topology of information exchange between AUVs is unconnected.

According to A2, the diagnostic areas of multiple obstacles are completely independent. This assumption precludes the inability of the AUV to determine which obstacle to avoid after entering the crossover area. Thus, each AUV will encounter only one obstacle at a given time.

4. Consensus Algorithm for Optimal Obstacle Avoidance

In this section, the consensus problem is expressed by the problem of optimal control. A closed consensus law of obstacle avoidance, which is a linear function of $(L \otimes I_m)X$ based on the local communication topology, is derived by the inverse optimal control method. \otimes denotes a Kronecker product that is used to extend the dimensions and I_m denotes the identity matrix of dimension m .

For the sake of presentation, the error state is defined as follows:

$$\hat{X} = [\hat{x}_1^T \hat{x}_2^T \dots \hat{x}_n^T]^T \triangleq X - X_{cs} \tag{4}$$

where $\mathbf{X}_{cs} = [\mathbf{1}_{1 \times n} \otimes \mathbf{x}_{cs}^T]^T$ denotes the ultimate consensus state. For example, for motion in space, $\mathbf{x}_{cs} = [\alpha_x \quad \alpha_y \quad \alpha_z]^T$, where α_x , α_y , and α_z express the ultimate consensus position of the x -axis, y -axis, and z -axis, respectively. Based on the property of the Laplacian \mathbf{L} in Equation (2), when all AUVs reach the consensus, we obtain

$$(\mathbf{L} \otimes \mathbf{I}_m)\mathbf{X}_{cs} = \mathbf{0}_{nm \times 1} \tag{5}$$

The ultimate consensus state \mathbf{X}_{cs} is constant at the moment and when the AUV reaches the consensus, the consensus law \mathbf{U} reaches zero.

Thus, the error of dynamics becomes

$$\dot{\hat{\mathbf{X}}} = \mathbf{U} \tag{6}$$

If the system (Equation (6)) is asymptotically stable, it will reach the consensus.

$$\begin{aligned} \min : J &= J_1 + J_2 + J_3 \\ \text{s.t. } \dot{\hat{\mathbf{X}}} &= \mathbf{U} \end{aligned} \tag{7}$$

The function of the optimal obstacle avoidance is constructed, the formula for which consists of three cost functions, where J_1 expresses the control effort cost, J_2 denotes the consensus cost, and J_3 indicates the obstacle avoidance cost.

First, the control effort cost is

$$J_1 = \int_0^\infty \mathbf{U}^T \mathbf{R}_1 \mathbf{U} dt \tag{8}$$

$$\mathbf{R}_1 = w_c^2 \mathbf{I}_n \otimes \mathbf{I}_m \tag{9}$$

In Equation (8), J_1 is a regular quadratic, and in Equation (9), \mathbf{R}_1 is a positive definite matrix. Furthermore, a scalar weighting parameter w_c is defined.

Second, the consensus cost is

$$J_2 = \int_0^\infty \hat{\mathbf{X}}^T \mathbf{R}_2 \hat{\mathbf{X}} dt = \int_0^\infty \hat{\mathbf{X}}^T (w_p^2 \mathbf{L}^2 \otimes \mathbf{I}_m) \hat{\mathbf{X}} dt \tag{10}$$

In Equation (10), the Laplacian matrix \mathbf{L} is established by the undirected and connected graph and it is symmetric. The weight of the consensus error is represented by w_p .

Proposition 1 ([32]). \mathbf{L}^2 is positive semidefinite, and when the graph is connected and undirected, $\mathbf{L}^2 \mathbf{1}_{n \times 1} = \mathbf{0}_{n \times 1}$.

Remark 1. Proposition 1 indicates that \mathbf{R}_2 is a positive semidefinite matrix. The \mathbf{R}_2 formula in Equation (10) can ensure that the optimal control law is the linear function of \mathbf{L} , and it is entirely dependent on the flow of information in the topology, as expressed by the proof of Theorem 1.

Finally, the obstacle avoidance cost is

$$J_3 = \int_0^\infty h(\hat{\mathbf{X}}) dt, \tag{11}$$

where $h(\hat{\mathbf{X}})$ is constructed from an inverse optimal control method using Theorem 1.

The following lemma is established for proving both the asymptotic stability and optimality of the obstacle avoidance consensus algorithm.

Lemma 1. A nonlinear controlled dynamical system [20] is modeled as

$$\dot{\hat{\mathbf{X}}}(t) = f(\hat{\mathbf{X}}(t), \mathbf{U}(t)), \hat{\mathbf{X}}(0) = \hat{\mathbf{X}}_0, t \geq 0, \tag{12}$$

where $f(\mathbf{0}, \mathbf{0}) = \mathbf{0}$ and the cost function is

$$J(\hat{X}_0, \mathbf{U}(\cdot)) \triangleq \int_0^\infty T(\hat{X}(t), \mathbf{U}(t)) dt. \tag{13}$$

In Equation (13), $\mathbf{U}(\cdot)$ denotes an admissible control.

The open sets are defined as $D \in \mathbb{R}^n$ and $\Omega \in \mathbb{R}^m$. Moreover, the continuous differentiable function $V : D \rightarrow \mathbb{R}$ and control law $\phi : D \rightarrow \Omega$ exist. Thus,

$$V(\mathbf{0}) = \mathbf{0} \tag{14}$$

$$\phi(\mathbf{0}) = \mathbf{0} \tag{15}$$

$$V(\hat{X}) > 0, \hat{X} \in D, \hat{X} \neq \mathbf{0} \tag{16}$$

$$V'(\hat{X})f(\hat{X}, \phi(\hat{X})) < 0, \hat{X} \in D, \hat{X} \neq \mathbf{0} \tag{17}$$

$$H(\hat{X}, \phi(\hat{X})) = 0, \hat{X} \in D \tag{18}$$

$$H(\hat{X}, \mathbf{U}) \geq 0, \hat{X} \in D, \mathbf{U} \in \Omega. \tag{19}$$

In Equation (19), $H(\hat{X}, \mathbf{U}) \triangleq T(\hat{X}, \mathbf{U}) + V'(\hat{X})f(\hat{X}, \mathbf{U})$ is the Hamiltonian function and $'$ indicates partial differentiation with respect to \hat{X} .

The state feedback control law has the following form:

$$\mathbf{U}(\cdot) = \phi(\hat{X}(\cdot)). \tag{20}$$

The solution $\hat{X}(t) \equiv \mathbf{0}$ of the closed-loop system is locally asymptotically stable and it has a neighborhood with the origin $D_0 \subset D$; thus,

$$J(\hat{X}_0, \phi(\hat{X}(\cdot))) = V(\hat{X}_0), \hat{X}_0 \in D_0. \tag{21}$$

Moreover, if $\hat{X}_0 \in D_0$, the feedback control $\mathbf{U}(\cdot) = \phi(\hat{X}(\cdot))$ minimizes $J(\hat{X}_0, \mathbf{U}(\cdot))$ so that

$$J(\hat{X}_0, \phi(\hat{X}(\cdot))) = \min_{\mathbf{U}(\cdot) \in S(\hat{X}_0)} J(\hat{X}_0, \mathbf{U}(\cdot)) \tag{22}$$

where $S(\hat{X}_0)$ represents the set of asymptotically stabilizing controllers for each initial condition $\hat{X}_0 \in D$. Finally,

if $D \in \mathbb{R}^n$, $\Omega \in \mathbb{R}^m$, and

$$V(\hat{X}) \rightarrow \infty \text{ as } \|\hat{X}\| \rightarrow \infty \tag{23}$$

the solution $\hat{X}(t) \equiv \mathbf{0}$ of the closed-loop system is globally asymptotically stable.

Proof. Omitted. See reference [23]. \square

This lemma emphasizes that the steady-state solution of the Hamilton–Jacobi–Bellman equation is a Lyapunov function for the nonlinear system, thereby ensuring the stability and optimality of the system. The following theorem expresses the main result of this study.

Theorem 1. For a system of MAUVs (3) that is established by the three hypotheses with parameters w_p and w_c , the feedback control law in which

$$\phi(\mathbf{X}) = -\frac{w_p}{w_c} (\mathbf{L} \otimes \mathbf{I}_m) \mathbf{X} - \frac{1}{2w_c^2} \mathbf{g}'(\mathbf{X}) \tag{24}$$

is an optimal control for the consensus problem (7) with

$$h(\hat{X}) = -\frac{w_p}{w_c} g'^T(\hat{X})(L \otimes I_m)\hat{X} + \frac{1}{4w_c^2} g'^T(\hat{X})g'(\hat{X}) \tag{25}$$

in Equation (9).

In Equation (25), the potential obstacle avoidance function $g(\hat{X})$ is defined as

$$g(\hat{X}) = \sum_{i=1}^n m(x_i) = g(X). \tag{26}$$

Furthermore,

$$m(x_i) = \begin{cases} \mathbf{0} & x_i \in \Pi \\ \left(\frac{R_j^2 - \|x_i - O_{bj}\|^2}{\|x_i - O_{bj}\|^2 - r_j^2} \right)^2 & x_i \in \Gamma_j, i = 1, \dots, n \\ \text{not defined} & x_i \in \Lambda_j \end{cases} \tag{27}$$

and

$$\begin{aligned} g'(\hat{X}) &= \begin{bmatrix} \left(\frac{dm(x_1)}{d\hat{x}_1} \right)^T & \left(\frac{dm(x_2)}{d\hat{x}_2} \right)^T & \dots & \left(\frac{dm(x_n)}{d\hat{x}_n} \right)^T \end{bmatrix}^T \\ &= \begin{bmatrix} \left(\frac{dm(x_1)}{dx_1} \right)^T & \left(\frac{dm(x_2)}{dx_2} \right)^T & \dots & \left(\frac{dm(x_n)}{dx_n} \right)^T \end{bmatrix}^T \\ &= g'(X) \end{aligned} \tag{28}$$

where $g'(\hat{X})$ means the derivative of $g'(X)$ for \hat{X} .

Moreover, when $X(t) \rightarrow X_{cs}$, the global asymptotic stability or consensus of the closed-loop system is guaranteed.

Proof. The following equations can be obtained using Lemma 1 for this optimal consensus problem:

$$T(\hat{X}, U) = \hat{X}^T R \hat{X} + h(\hat{X}) + U^T R_1 U \tag{29}$$

$$f(\hat{X}, U) = U \tag{30}$$

where $f(\mathbf{0}_{nm \times 1}, \mathbf{0}_{nm \times 1}) = \mathbf{0}_{nm \times 1}$. □

By selecting $V(\hat{X})$, which is an applicable Lyapunov function then

$$V(\hat{X}) = \hat{X}^T P \hat{X} + g(\hat{X}) \tag{31}$$

P is the solution of the Riccati equation, which is expressed later.

For the function in Equation (31), $V(\hat{X})$ should be a valid Lyapunov function. It must be continuously differentiable with respect to \hat{X} , and in this case, $g(\hat{X})$ is continuously differentiable with respect to \hat{X} . It can be observed from Equations (26) and (27) that in the safety area Θ , $m(x_i)$ will be continuously differentiable. If $m(x_i)$ and $\frac{dm(x_i)}{dx_i}$ are continuous at the boundary of the diagnostic zone, i.e., $\|x_i - O_{bj}\| = R_j$, this is true. As Equation (27) means that $\lim_{\|x_i - O_{bj}\| \rightarrow R_j^-} m(x_i) = \mathbf{0} = \lim_{\|x_i - O_{bj}\| \rightarrow R_j^+} m(x_i)$, $m(x_i)$ is continuous at $\|x_i - O_{bj}\| = R_j$, and thus, continuous over Θ . Furthermore,

$$\frac{dm(x_i)}{dx_i} = \begin{cases} \mathbf{0} & x_i \in \Pi \\ \frac{-4(R_j^2 - r_j^2)(R_j^2 - \|x_i - O_{bj}\|^2)}{(\|x_i - O_{bj}\|^2 - r_j^2)^3} (x_i - O_{bj}) & x_i \in \Gamma_j \\ \text{not defined} & x_i \in \Lambda_j \end{cases} \tag{32}$$

Therefore, $\lim_{\|x_i - O_{bj}\| \rightarrow R_j^-} \frac{dm(x_i)}{dx_i} = \mathbf{0}_{m \times 1} = \lim_{\|x_i - O_{bj}\| \rightarrow R_j^+} \frac{dm(x_i)}{dx_i}$, which means that $\frac{dm(x_i)}{dx_i}$ is continuous at $\|x_i - O_{bj}\| = R_j$, and thus, continuous over safety area Θ .

As a result, $g(\hat{X})$ and $V(\hat{X})$ are continuously differentiable for \hat{X} in safety area Θ . The Hamiltonian for the consensus problem becomes

$$\begin{aligned} H(\hat{X}, U) &= T(\hat{X}, U) + V^T(\hat{X})f(\hat{X}, U) \\ &= \hat{X}R_2\hat{X} + h(\hat{X}) + U^TR_1U + [2\hat{X}^TP + g^T(\hat{X})]U \end{aligned} \tag{33}$$

Setting $(\partial/\partial U)H(\hat{X}, U) = \mathbf{0}$ results in the optimal control law:

$$U^* = \phi(\hat{X}) = -\frac{1}{2}R_1^{-1}V'(\hat{X}) = -R_1^{-1}P\hat{X} - \frac{1}{2}R_1^{-1}g'(\hat{X}). \tag{34}$$

From Equation (33), it follows that

$$\begin{aligned} V^T(\hat{X})f(\hat{X}, U) &= -2\hat{X}^TPR_1^{-1}P\hat{X} - \hat{X}PR_1^{-1}g'(\hat{X}) \\ &\quad - g^T(\hat{X})R_1^{-1}P\hat{X} - \frac{1}{2}g^T(\hat{X})R_1^{-1}g'(\hat{X}) \end{aligned} \tag{35}$$

Substituting Equations (33) and (34) into (32) yields

$$\begin{aligned} H(\hat{X}, \phi(\hat{X})) &= \hat{X}^T(R_2 - PR_1^{-1}P)\hat{X} - g^T(\hat{X})R_1^{-1}P\hat{X} \\ &\quad + h(\hat{X}) - \frac{1}{4}g^T(\hat{X})R_1^{-1}g'(\hat{X}) \end{aligned} \tag{36}$$

For the consensus problem (7), we can prove that the control law (34) is an optimal solution using Lemma 1, but it is necessary to verify conditions (14) to (19). By satisfying condition (18) or causing Equation (36) to be zero, we can obtain

$$R_2 - PR_1^{-1}P = \mathbf{0} \tag{37}$$

and demand

$$-g^T(\hat{X})R_1^{-1}P\hat{X} + h(\hat{X}) - \frac{1}{4}g^T(\hat{X})R_1^{-1}g'(\hat{X}) = \mathbf{0}. \tag{38}$$

Using Equations (34) and (36)–(38), it can be observed that

$$\begin{aligned} H(\hat{X}, U, V^T(\hat{X})) &= U^TR_1U + h(\hat{X}) + \hat{X}^TR_2\hat{X} + (2\hat{X}^TP + g^T(\hat{X}))U \\ &= U^TR_1U + h(\hat{X}) + \hat{X}^TR_2\hat{X} + (2\hat{X}^TP + g^T(\hat{X}))U \\ &\quad - \hat{X}^T(R_2 - PR_1^{-1}P)\hat{X} \text{ (using Equation (37))} \\ &= U^TR_1U + h(\hat{X}) + g^T(\hat{X})U + 2\hat{X}^TPU + \hat{X}^TPR_1^{-1}P\hat{X} \\ &= U^TR_1U + \frac{1}{4}g^T(\hat{X})R_1^{-1}g'(\hat{X}) + g^T(\hat{X})R_1^{-1}P\hat{X} \\ &\quad + \hat{X}^TPR_1^{-1}P\hat{X} + (2\hat{X}^TP + g^T(\hat{X}))U \text{ (using Equation (38))} \\ &= U^TR_1U + \frac{1}{4}(2\hat{X}^TP + g^T(\hat{X}))R_1^{-1}(2\hat{X}^TP + g^T(\hat{X}))T \\ &\quad + (2\hat{X}^TP + g^T(\hat{X}))U \\ &= U^TR_1U + \frac{1}{4}V^T(\hat{X})R_1^{-1}V'(\hat{X}) + U^TV'(\hat{X}) \\ &= U^TR_1U + \phi(\hat{X})^TR_1\phi(\hat{X}) \\ &\quad - 2U^TR_1\phi(\hat{X}) \text{ (using Equation (34))} \\ &= [U - \phi(\hat{X})]^TR_1[U - \phi(\hat{X})] \geq 0 \end{aligned} \tag{39}$$

and condition (19) is validated.

By substituting the expressions of R_1, R_2 in Equation (37), a candidate function for P is obtained:

$$P = w_p w_c L \otimes I_m \tag{40}$$

such that the Lyapunov function (31) becomes

$$\begin{aligned}
 V(\hat{X}) &= g(\hat{X}) + \hat{X}^T P \hat{X} \\
 &= \begin{cases} w_p w_c X^T (L \otimes I_m) X & x_i \in \Pi \\ g(X) + w_p w_c X^T (L \otimes I_m) X & x_i \in \Gamma_j \\ \text{not defined} & x_i \in \Lambda_j \end{cases} \quad (41)
 \end{aligned}$$

Note that the property of L in Equation (5) is used to convert $V(\hat{X})$ into $V(X)$. If $\hat{X} \neq 0$ or $X \neq X_{cs}$, based on the property of the Laplacian matrix, $X^T (L \otimes I_m) X$ will not be zero, but positive. Note that when $X = 0$ can lead to $X^T (L \otimes I_m) X = 0$, this is a special case of $X = X_{cs}$ and $X_{cs} = 0$, which also implies $\hat{X} = 0$. Therefore, $X^T (L \otimes I_m) X > 0$ if $\hat{X} \neq 0$. Furthermore, $g(X)$ is defined by Equations (26) and (27), and it is easily shown that $g(X) > 0$. When $w_p w_c X^T (L \otimes I_m) X + g(X) > 0$ for $\hat{X} \neq 0$, condition (16), i.e., $V(\hat{X}) > 0$ for $\hat{X} \neq 0$, can be met.

Subsequently, $h(\hat{X})$ in J_3 is constructed by solving Equation (37):

$$h(\hat{X}) = \frac{w_p}{w_c} g^T(\hat{X}) (L \otimes I_m) \hat{X} + \frac{1}{4w_c^2} g'^T(\hat{X}) g'(\hat{X}) \quad (42)$$

which becomes (25). The selection of appropriate values for the weighting parameters can guarantee $h(\hat{X}) > 0$. When w_c is valuated, a sufficiently small w_p can always be determined for the positive-definite term $\frac{1}{4w_c^2} g'^T(\hat{X}) g'(\hat{X})$ to control the sign-indefinite term $\frac{w_p}{w_c} g^T(\hat{X}) (L \otimes I_m) \hat{X}$.

Let

$$\begin{aligned}
 V^T(\hat{X}) f(\hat{X}, \phi(\hat{X})) &= -[\hat{X}^T R_2 \hat{X} + h(\hat{X}) \\
 &\quad + (\hat{X}^T P + \frac{1}{2} g'^T(\hat{X})) \times R_1^{-1} (P \hat{X} + \frac{1}{2} g^T(\hat{X}))] \quad (43)
 \end{aligned}$$

using Equations (37) and (38), with Equation (35).

If $\hat{X}^T R_1 \hat{X} \geq 0$, $h(\hat{X}) \geq 0$ and $(\hat{X}^T P + \frac{1}{2} g'^T(\hat{X})) R_1^{-1} (P \hat{X} + \frac{1}{2} g^T(\hat{X})) > 0$ when $\hat{X} \neq 0$. Thus, condition (17) can be satisfied.

Conditions (14) and (15) still need to be verified. According to Equations (31) and (34), when $\hat{X} = 0$, $g(\hat{X}) = 0$, and $g'(\hat{X}) = 0$, conditions (14) and (15) are satisfied. According to Equations (24), (28) and (32), if all AUVs assemble in the reaction area, the avoidance force of each AUV will not be zero and all AUVs will leave the reaction area until a new consensus point is reached. If the consensus point $\hat{X} = 0$ is beyond the reaction area of the obstacle, it can easily be observed that $g(\hat{X}) = 0$ and $g'(\hat{X}) = 0$; thus, conditions (14) and (15) are satisfied.

The optimal control law in Equation (24) can be obtained using Equation (40) and substituting $\hat{X} = X - X_{cs}$ into (34). Note that, owing to Equation (5), the part containing the ultimate consensus state X_{cs} becomes zero. Thus, the control law (24) depends on X and not X_{cs} . This satisfies the expectations because X_{cs} is not a priori.

At present, conditions (14) to (19) have been satisfied. Thus, according to Lemma 1, the control law (24) is the optimal control law for problem (7) in the sense of Equations (21) and (22), and the closed-loop system is asymptotically stable. Thus, $X = X_{cs}$ and the consensus is achieved.

Moreover, it can easily be determined from Equation (31) that $V(\hat{X}) \rightarrow \infty$ as $\hat{X} = 0$. The closed-loop system is globally asymptotically stable. Note that the collision area Λ_j is also excluded in the globally asymptotic stability area because no AUV exists to begin to avoid the obstacle.

Remark 2. Owing to the proof of Theorem 1, noting that the optimal consensus algorithm is studied by the method of inverse optimal control, as the function $h(\hat{X})$ in J_3 is not specified a priori, it is constructed using the optimality condition in Equation (38). The obstacle avoidance can be understood according to $h(\hat{X})$ and Equations (25), (27) and (29): if the AUV is beyond the

diagnostic zone, $h(\hat{X}) = 0$, and thus, $J_3 = 0$; if the AUV is in the reaction area and close to the obstacle, the denominator $\|x_i - O_{bj}\|^2 - r_j^2$ in $h(\hat{X})$ (see $m(x_i)$ in Equation (27)) will reach zero and J_3 will increase. This indicates that the AUV is leaving an obstacle. Therefore, the obstacle avoidance ability is guaranteed according to the asymptotic stability and the optimality of the system can be ensured by Theorem 1.

Remark 3. We summarize the optimal consensus algorithm. First, w_p and w_c are changeable weighting parameters, where w_p influences the consensus error and w_c influences the control effort. Second, the condition of $h(\hat{X}) \geq 0$ must be ensured by these parameters. The changing of these parameters is the same as in the conventional LQR problem for changing the weighting matrices Q and R :

$$\int_0^\infty [\hat{X}^T Q \hat{X} + U^T R U] dt. \tag{44}$$

In a linear single-integrator system, it is not complicated to change w_p and w_c . However, the cost function of the obstacle avoidance should be a nonquadratic nonlinear function, so the linear optimal control problem differs from the LQR. As only two parts exist in $h(\hat{X})$, the basic principles of the selection of the two parameters are as follows: the consensus error needs to be balanced, and for a given w_c , the control effort also needs to select a sufficiently small weighting parameter w_p such that the sign-indefinite term $\frac{w_p}{w_c} g^T(\hat{X})(L \otimes I_m) \hat{X}$ is always less than the positive term $\frac{1}{4w_c^2} g^T(\hat{X}) g'(\hat{X})$ to obtain the condition $h(\hat{X}) \geq 0$.

Remark 4. According to $\phi(X)$ in Equation (24), the optimal control law only needs to contain two parts: the consensus law and obstacle avoidance law.

The consensus law of the AUVs is a linear function of $(L \otimes I_m)X$. Only the local information between the AUVs is required and they exchange the information using the communication topology, instead of the information of all AUVs. Therefore, $g'(X)$ in the optimal control law only requires local information for execution.

5. Simulation

The consensus law of the optimal obstacle avoidance was verified using a simulation environment. Consider the scene of five AUVs moving in space ($m = 3$) in Figure 1. According to the definition, L can be expressed as follows:

$$L = \begin{bmatrix} 2 & -1 & 0 & 0 & -1 \\ -1 & 2 & -1 & 0 & 0 \\ 0 & -1 & 2 & -1 & 0 \\ 0 & 0 & -1 & 2 & -1 \\ -1 & 0 & 0 & -1 & 2 \end{bmatrix}. \tag{45}$$

The initial positions of the five AUVs are given by (1, 2, 3), (30, 30, 30), (2, 14, 0), (15, 30, 25), and (30, 18, 20). We let $w_p = 0.8$ and $w_c = 4$.

5.1. Consensus of No Obstacles in AUV Trajectories

It is assumed that the obstacle appears at (14, 17, 20) and that it does not appear on the trajectory of any AUV. Assume that the collision zone (obstacle radius) is $r_1 = 0.5$ and the radius of the diagnostic zone is $R_1 = 1$. Figures 3 and 4 depict the motion simulation results of the five AUVs according to the proposed optimal consensus law. Figure 3 show the trajectories of the AUVs in space and the projections of the trajectories onto a certain plane, respectively. Figure 4 shows the optimal control input and the time history of the positions. The ultimate consensus point is located at (15.59, 18.8, 15.59).

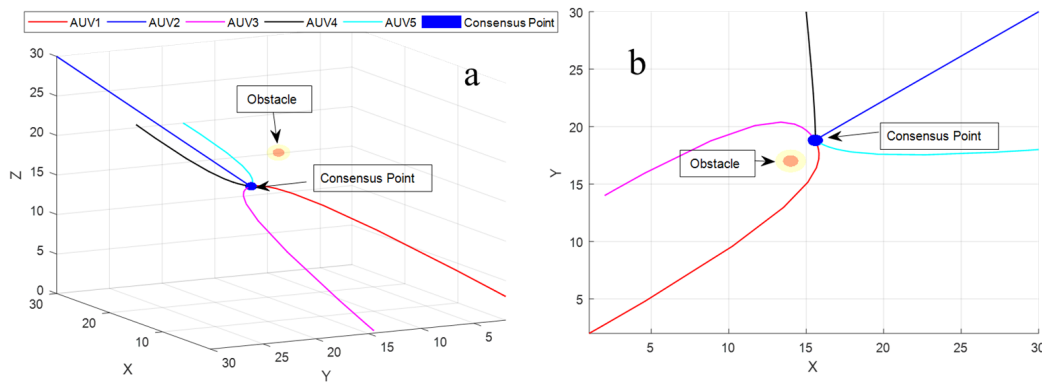


Figure 3. (a) Consensus trajectories of five AUVs with no obstacles. (b) Consensus trajectories of five AUVs with no obstacles in X–Y plane.

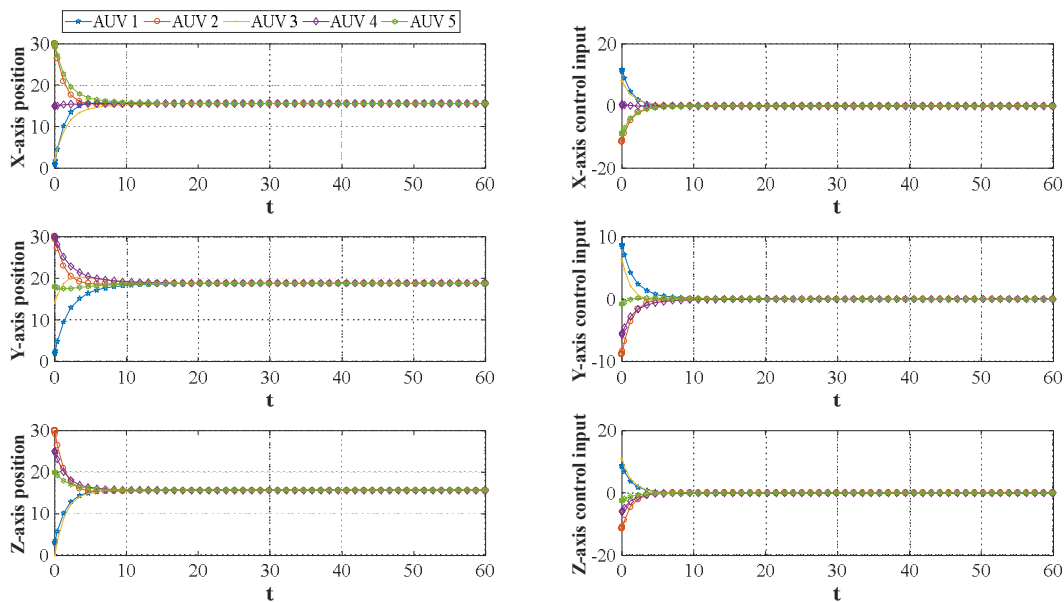


Figure 4. Time histories of positions and control inputs of five AUVs with no obstacles in trajectories.

As all AUVs are beyond the diagnostic zone, the obstacle avoidance cost function $h(\hat{X}) = 0$ (Equation (10)). Thus, the problem becomes a normal consensus problem.

5.2. Consensus of Obstacles in AUV Trajectories

In this part, we consider different places and times of the appearance of obstacles. Assume that the first obstacle appears in the trajectory of AUV 2 (23, 24, 22), the radius of the obstacle is $r_1 = 0.7$, and the diagnostic zone is $R_1 = 1.5$. The second obstacle at (14, 17, 20) does not exist in the trajectory of any AUV. The final obstacle is assumed to appear in the trajectory of AUV 1 at (7, 7, 7). The radius and diagnostic area of the obstacle are $r_1 = 1$ and $R_1 = 2.5$, respectively. Figure 5 depict the simulation results.

It can be observed from Figure 5 that all AUVs could avoid multiple obstacles on the trajectory and finally reached a consensus point (15.28, 18.59, 15.69), which differed from the previous consensus point (15.59, 18.8, 15.59). Figure 6, which shows the control input of the AUVs and time history of the position, respectively, reveals that the proposed optimal control law could achieve consensus as well as multi-obstacle avoidance.

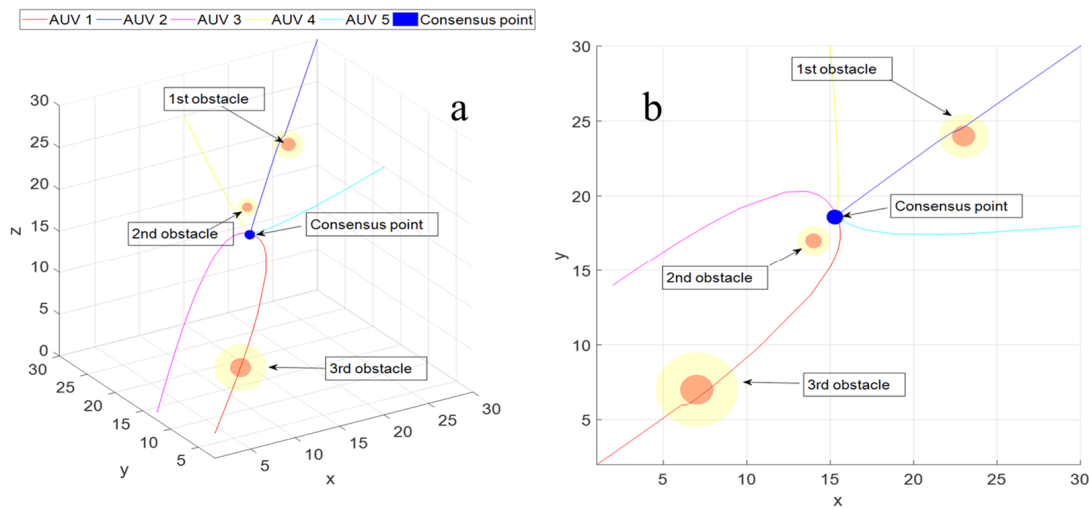


Figure 5. (a) Consistent trajectories of five AUVs with three obstacles, where obstacles appear in the trajectories of AUV 1 and AUV 2. (b) Consistent trajectories of five AUVs with multiple obstacles, where obstacles appear in the trajectories of AUV 1 and AUV 2 in the Y-Z plane.

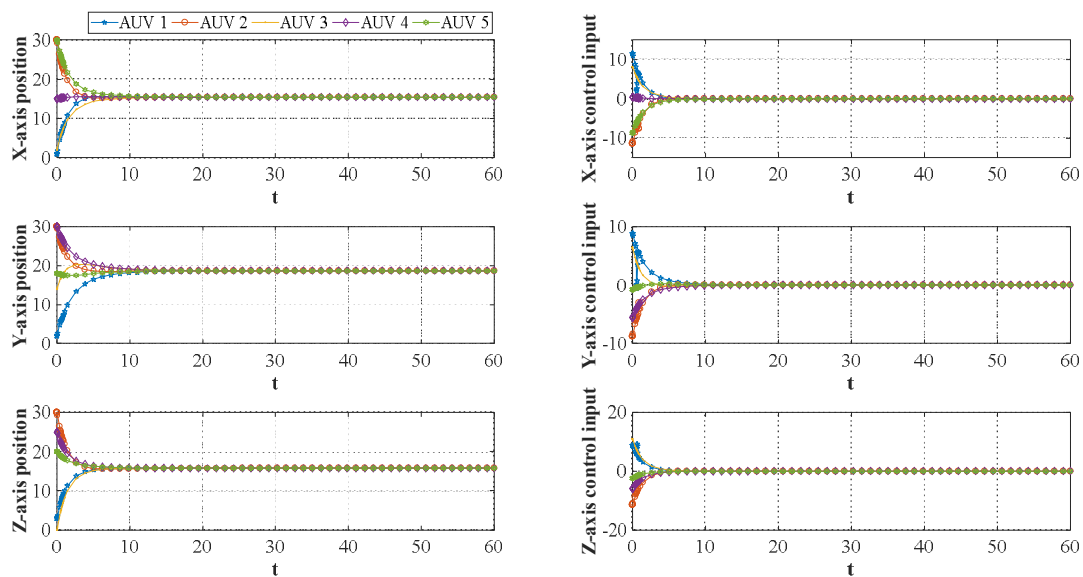


Figure 6. Time histories of positions and controls of five AUVs with multiple obstacles.

6. Experiment

We carried out a sea experiment in November 2022 (Figure 7). We established two robots: AUV 0 was used for AUV charging and data interaction, and AUV 1 could move freely. AUV 0 and AUV 1 had the same control system, but AUV 0 did not carry a propeller, so it was set as an AUV with a sailing speed of zero. The two robots could be regarded as heterogeneous AUVs, and the entire experimental environment was 1500 m underwater. The experimental process was as outlined below.

1. Positioning and communication devices were installed on the AUVs. Each AUV had the ability to exchange information with the other.
2. AUV 1 was placed into the water.
3. AUV 0 was placed into the water 300 m from AUV 1.
4. When the two devices reached the sea floor, the position of the two AUVs was determined by the ultra-short baseline equipment on board and the positions were transmitted to AUV 1 and AUV 0 via acoustic communication.

5. AUV 1 and AUV 0 exchanged information at 8 s intervals through their own acoustic communication devices.
6. AUV 1 moved towards AUV 0, and finally, AUV 1 appeared in front of AUV 0.

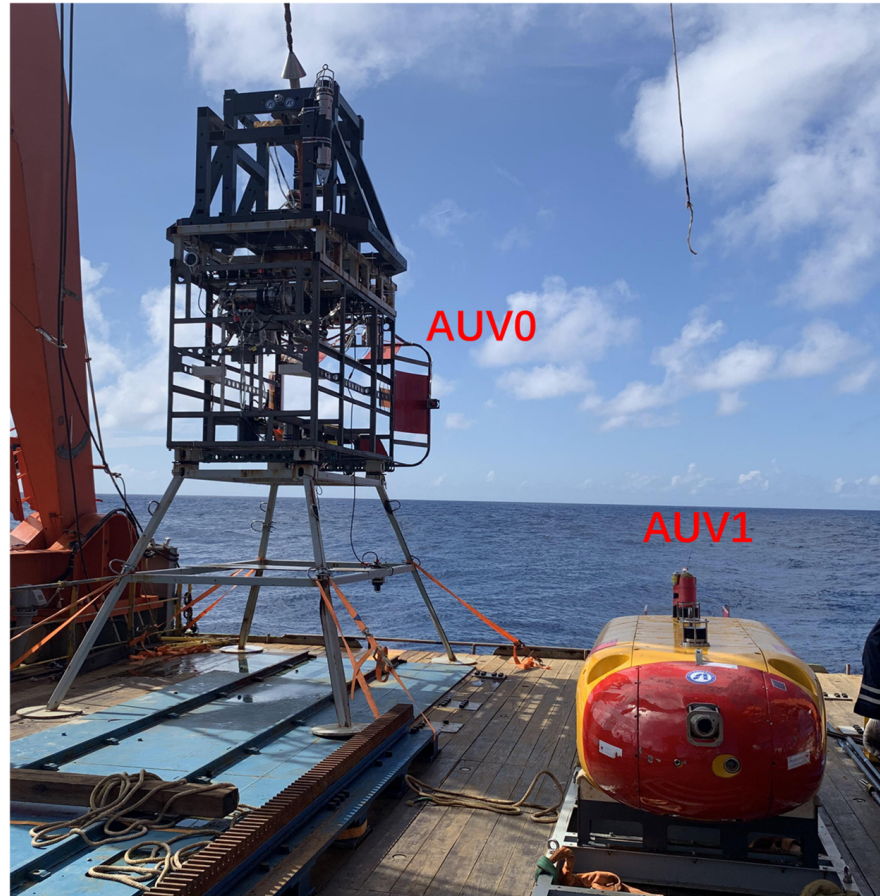


Figure 7. Two AUVs in the experiment.

It can be observed from Figure 8 that AUV 1 descended to the seabed in the form of a spiral wire, and AUV 0 was laid into the water during the process of AUV 1 diving. As indicated in Figure 9, The red sphere means the position information of AUV1 from AUV1; each two minutes the AUV0 obtains the information. The green sphere means the position information of AUV1 from AUV0 by the position system; each eight seconds the AUV0 obtains the information. The inset on the top right means the view from the above camera in the software. From the figure we obtain the trajectory of AUV1 moved toward AUV0. AUV 1 approached AUV 0 after exchanging information with AUV 0, and the entire process was completely automatic. The system realized the collection of heterogeneous AUVs through the algorithms.

Figure 10 presents selected screenshots of a certain period to verify that AUV 1 appeared in front of AUV 0 and could proceed to the next step. It describes the final progress of the system reaching consensus, from the view of AUV0; AUV1 was moving towards AUV0 through their information and when the AUV1 moved, it lit the red light, the inset on the top left means time.

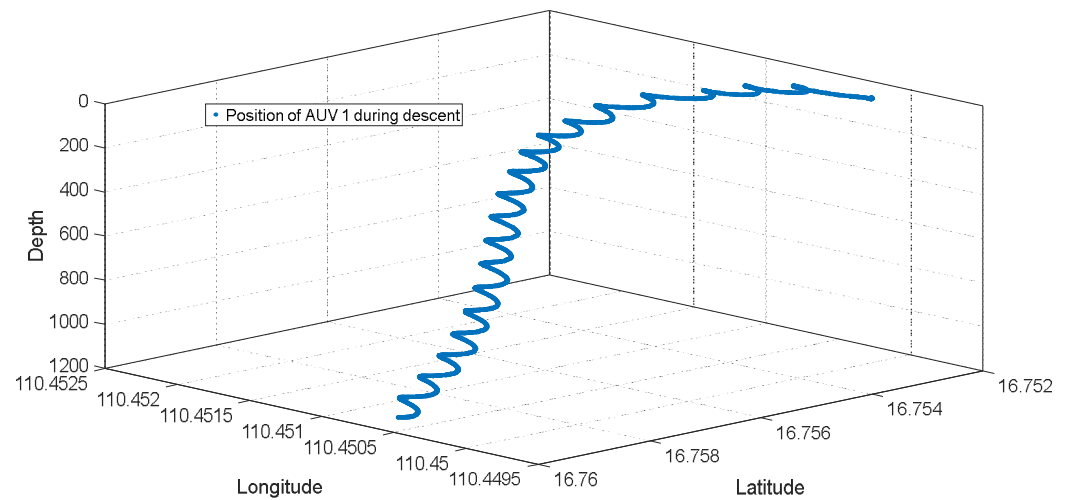


Figure 8. Trajectory of AUV 1 during descent.

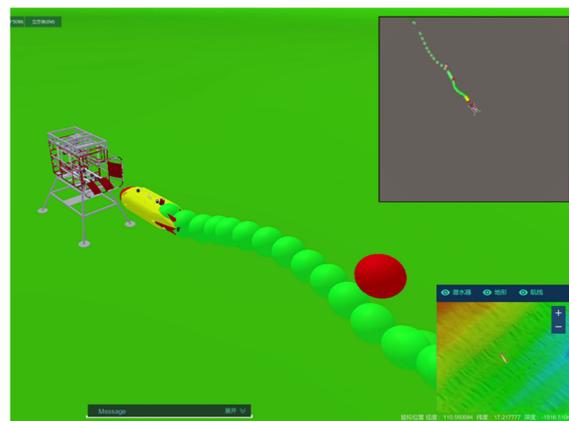


Figure 9. Process data of AUV 1 approaching AUV 0.



Figure 10. View of AUV 1 from AUV 0.

7. Conclusions

This paper studied the consensus and obstacle avoidance control problems of multiple AUVs under ocean environment with static obstacles. A novel control approach was developed to achieve multi-AUV consensus and to have the minimal obstacle avoidance cost. In the inverse optimal control approach, a novel nonquadratic obstacle avoidance cost function was constructed; the control law can be obtained from local information from other AUVs by the communication topology. The system of multi-AUVs had globally asymptotic stability and optimality. The simulation results as well as the experiments show that the multi-AUVs can effectively avoid obstacles while maintaining the desired position.

The multi-AUV consensus control problem under practical conditions was studied in part. At the same time, the communication issues between AUVs, such as delay, noise, sampling rate, etc., were not considered in this article. However, in practical applications, the communication directly determines whether the AUVs can achieve the desired formation shape, which should be improved in further research.

Author Contributions: Conceptualization, L.W.; methodology, G.S.; software, G.S.; validation, G.S. and H.X.; writing—original draft preparation, G.S.; writing—review and editing, H.X.; visualization, G.S.; supervision, H.X.; project administration, H.X.; funding acquisition, H.X. All authors have read and agreed to the published version of the manuscript.

Funding: This work was supported by the Strategic Priority Research Program of the Chinese Academy of Sciences [grant number XDA22040103].

Institutional Review Board Statement: Not applicable.

Informed Consent Statement: Not applicable.

Data Availability Statement: Data are contained within the article.

Acknowledgments: The research was completed at Harbin Engineering University and Shenyang Institute of Automation (SIA), Chinese Academy of Sciences. At the same time, we would like to acknowledge the technical support and collaboration of our AUV team.

Conflicts of Interest: The authors declare no conflict of interest.

References

1. Hodges, B.A.; Fratantoni, D.M. AUV observations of the diurnal surface layer in the north Atlantic salinity maximum. *J. Phys. Oceanogr.* **2014**, *44*, 1595–1604. [[CrossRef](#)]
2. Yan, J.; Yang, X.; Luo, X.; Chen, C. Energy-efficient data collection over AUV-assisted underwater acoustic sensor network. *IEEE Syst. J.* **2018**, *12*, 3519–3530. [[CrossRef](#)]
3. Antonelli, G.; Jesus, S.; Kebkal, K.; Pascoal, A.; Polani, D.; Pollini, L.; Caffaz, A.; Casalino, G.; Volpi, N.C.; de Jong, I.B.; et al. The Widely Scalable Mobile Underwater Sonar Technology (WiMUST) H2020 Project: First year status. In Proceedings of the OCEANS 2016, Shanghai, China, 10–13 April 2016; pp. 1–8.
4. Poulsen, A.J.; Eickstedt, D.P.L.; Ianniello, J.P. Bearing stabilization and tracking for an AUV with an acoustic line array. In Proceedings of the OCEANS 2006, Boston, MA, USA, 18–21 September 2006; pp. 1–6.
5. Liang, Q.; Sun, T.; Wang, D. Reliability indexes for multi-AUV cooperative systems. *J. Syst. Eng. Electron.* **2017**, *28*, 179–186. [[CrossRef](#)]
6. Joordens, M.A.; Jamshidi, M. Consensus control for a system of underwater swarm robots. *IEEE Syst. J.* **2010**, *4*, 65–73. [[CrossRef](#)]
7. Olfati-Saber, R.; Murray, R.M. Consensus problems in networks of agents with switching topology and time-delays. *IEEE Trans. Autom. Control* **2004**, *49*, 1520–1533. [[CrossRef](#)]
8. Jadbabaie, A.; Lin, J.; Morse, A.S. Coordination of groups of mobile autonomous agents using nearest neighbor rules. *IEEE Trans. Autom. Control* **2003**, *48*, 988–1001. [[CrossRef](#)]
9. Ren, W.; Beard, R.W. Consensus seeking in multiagent systems under dynamically changing interaction topologies. *IEEE Trans. Autom. Control* **2005**, *50*, 655–661. [[CrossRef](#)]
10. Yu, W.; Chen, G.; Cao, M. Some necessary and sufficient conditions for second-order consensus in multi-agent dynamical systems. *Automatica* **2010**, *46*, 1089–1095. [[CrossRef](#)]
11. Yu, W.; Chen, G.; Ren, W.; Kurths, J.; Zheng, W.X. Distributed higher order consensus protocols in multiagent dynamical systems. *IEEE Trans. Circuits Syst. I Regul. Pap.* **2011**, *58*, 1924–1932. [[CrossRef](#)]
12. Zhang, H.; Lewis, F.L.; Das, A. Optimal design for synchronization of cooperative systems: State feedback, observer and output feedback. *IEEE Trans. Autom. Control* **2011**, *56*, 1948–1952. [[CrossRef](#)]
13. Yu, Z.; Jiang, H.; Hu, C.; Yu, J. Necessary and sufficient conditions for consensus of fractional-order multiagent systems via sampled-data control. *IEEE Trans. Cybern.* **2017**, *47*, 1892–1901. [[CrossRef](#)] [[PubMed](#)]
14. Xiao, L.; Boyd, S. Fast linear iterations for distributed averaging. *Syst. Control Lett.* **2004**, *53*, 65–78. [[CrossRef](#)]
15. Kim, Y.; Mesbahi, M. On maximizing the second smallest eigenvalue of a state-dependent graph Laplacian. *IEEE Trans. Autom. Control* **2006**, *51*, 116–120. [[CrossRef](#)]
16. Delvenne, J.C.; Carli, R.; Zampieri, S. Optimal strategies in the average consensus problem. In Proceedings of the 2007 46th IEEE Conference on Decision and Control, New Orleans, LA, USA, 12–14 December 2007; pp. 2498–2503.
17. Semsar-Kazerooni, E.; Khorasani, K. An LMI approach to optimal consensus seeking in multi-agent systems. In Proceedings of the 2009 American Control Conference, Saint Louis, MO, USA, 10–12 June 2009; pp. 4519–4524.

18. Cao, Y.; Ren, W. Optimal linear-consensus algorithms: An LQR perspective. *IEEE Trans. Syst. Man Cybern. B Cybern.* **2010**, *40*, 819–830.
19. Alex, O.; Tsitsiklis, J.N. Convergence Speed in Distributed Consensus and Control. *SIAM Rev. SIAM* **2006**, *53*, 747–772.
20. Bradley, R. Reaching a consensus. *Soc. Choice Welf.* **2007**, *29*, 609–632. [[CrossRef](#)]
21. Lynch, N.A. *Distributed Algorithms*; Morgan Kaufmann: Burlington, MA, USA, 1996.
22. Vicsek, T.; Czirok, A.; Ben-Jacob, E.; Cohen, I.; Shochet, O. Novel type of phase transition in a system of self-driven particles. *Phys. Rev. Lett.* **1995**, *75*, 1226–1229. [[CrossRef](#)] [[PubMed](#)]
23. Bernstein, D.S. Nonquadratic cost and nonlinear feedback control. *Int. J. Robust Nonlinear Control* **1993**, *3*, 211–229. [[CrossRef](#)]
24. Lin, G.H.; Zhang, J.; Liu, Z.H. Hybrid Particle Swarm Optimization with Differential Evolution for Numerical and Engineering Optimization. *Int. J. Autom. Comput.* **2018**, *1*, 103–114. [[CrossRef](#)]
25. Zhang, H.; Hu, J.; Liu, H.; Yu, X.; Liu, F. Recursive state estimation for time-varying complex networks subject to missing measurements and stochastic inner coupling under random access protocol. *Neurocomputing* **2019**, *346*, 48–57. [[CrossRef](#)]
26. Zhang, W.; Zeng, J.; Yan, Z.; Wei, S.; Tian, W. Leader-following consensus of discrete-time multi-AUV recovery system with time-varying delay. *Ocean Eng.* **2021**, *219*, 108258. [[CrossRef](#)]
27. Yan, Z.; Yue, L.; Zhou, J.; Pan, X.; Zhang, C. Formation coordination control of leaderless multi-AUV system with double independent communication topology and non-convex control input constraints. *J. Mar. Sci. Eng.* **2023**, *11*, 107. [[CrossRef](#)]
28. Chen, K.; Luo, G.; Zhou, H.; Zhao, D. An improved event-triggered control method based on consistency algorithm in heterogeneous AUV swarm under communication delay. In Proceedings of the Bio-Inspired Computing: Theories and Applications: 16th International Conference, BIC-TA 2021, Taiyuan, China, 17–19 December 2021; Springer: Berlin/Heidelberg, Germany, 2022; pp. 206–221.
29. Shi, X.; Cao, J.; Wen, G.; Perc, M. Finite-time consensus of opinion dynamics and its applications to distributed optimization over digraph. *IEEE Trans. Cybern.* **2019**, *49*, 3767–3779. [[CrossRef](#)] [[PubMed](#)]
30. Nair, R.R.; Behera, L.; Kumar, S. Event-triggered finite-time integral sliding mode controller for consensus-based formation of multirobot systems with disturbances. *IEEE Trans. Control Syst. Technol.* **2019**, *27*, 39–47. [[CrossRef](#)]
31. Cai, Y.; Zhang, H.; Liu, Y.; He, Q. Distributed bipartite finite-time event-triggered output consensus for heterogeneous linear multiagent systems under directed signed communication topology. *Appl. Math. Comput.* **2020**, *378*, 125162. [[CrossRef](#)]
32. Bernstein, D.S. *Matrix Mathematics*; Princeton University Press: Princeton, NJ, USA, 2005; p. 295.

Disclaimer/Publisher’s Note: The statements, opinions and data contained in all publications are solely those of the individual author(s) and contributor(s) and not of MDPI and/or the editor(s). MDPI and/or the editor(s) disclaim responsibility for any injury to people or property resulting from any ideas, methods, instructions or products referred to in the content.